Aggregated LDL and lipid dispersions induce lysosomal cholesteryl ester accumulation in macrophage foam cells

Evelyn E. Griffin,* Jody C. Ullery,* Brian E. Cox,* and W. Gray Jerome[1,*,†]

Departments of Pathology* and Cancer Biology†, Vanderbilt University School of Medicine, Nashville, TN 37232

Abstract **Macrophage foam cells in atherosclerotic lesions accumulate substantial cholesterol stores within large, swollen lysosomes. Previous studies with mildly oxidized low density lipoprotein (OxLDL)-treated THP-1 macrophages suggest an initial buildup of free cholesterol (FC), followed by an inhibition of lysosomal cholesteryl ester (CE) hydrolysis and a subsequent lysosomal accumulation of unhydrolyzed lipoprotein CE. We examined whether other potential sources of cholesterol found within atherosclerotic lesions could also induce similar lysosomal accumulation. Biochemical analysis combined with microscopic analysis showed that treatment of THP-1 macrophages with aggregated low density lipoprotein (AggLDL) or CE-rich lipid dispersions (DISP) produced a similar lysosomal accumulation of both FC and CE. Cotreatment with an ACAT inhibitor, CP113,818, confirmed that the CE accumulation was primarily the result of the inhibition of lysosomal CE hydrolysis. The rate of unhydrolyzed CE buildup was more rapid with DISP than with AggLDL. However, with both treatments, FC appeared to accumulate in lysosomes before the inhibition in hydrolysis and CE accumulation, a sequence shared with mildly OxLDL. Thus, lysosomal accumulation of FC and CE can be attributable to more general mechanisms than just the inhibition of hydrolysis by oxidized lipids.**—Griffin, E. E., J. C. Ullery, B. E. Cox, and W. G. Jerome. **Aggregated LDL and lipid dispersions induce lysosomal cholesteryl ester accumulation in macrophage foam cells.** ***J. Lipid Res.*** **2005.** 46: **2052–2060.**

Supplementary key words atherosclerosis • lysosome • microscopy • low density lipoprotein

A characteristic feature of early atherosclerotic lesions is the presence of lipid-laden macrophage foam cells (1). Atherosclerotic foam cells derive the majority of their lipid from endocytic uptake of modified lipoproteins and other extracellular lipid particles (2–4). Lipoprotein modifications include acetylation, oxidation, and aggregation (2, 5, 6). Additionally, the atherosclerotic lesion extracellular milieu is rich in matrix components and lipid complexes also capable of stimulating cholesterol accumulation (4, 7). Thus, macrophage foam cells potentially can form through the accumulation of several different sources of modified particles.

Normally, internalized lipid is delivered to lysosomes for degradation. In lysosomes, cholesteryl ester (CE) can be hydrolyzed to unesterified (free) cholesterol (FC), which can then be transported out of lysosomes (8). Excess extralysosomal FC is usually reesterified to a fatty acid by ACAT and stored as CE in cytoplasmic inclusions (9). However, as atherosclerotic lesions develop and transit from a fatty streak to a fibrous plaque, FC and CE accumulate in lysosomes (10, 11). Thus, atherosclerosis has been described by some researchers as a modified lysosomal storage disease, and studies suggest an involvement of lysosomes in atherosclerotic pathology (12–15).

Although it is clear that lipoproteins must be modified to induce foam cells, not all modifications produce the same patterns of cholesterol accumulation. Cell culture studies involving oxidatively modified low density lipoproteins (OxLDL) indicate a role of lysosomes in cholesterol accumulation. In contrast, studies with acetylated low density lipoprotein (AcLDL) show that cholesterol from this source accumulates in ACAT-derived CE in cytoplasmic inclusions (16–18). Previous studies in our laboratory have also demonstrated an initial induction of lysosomal FC accumulation as a result of treatment with mildly OxLDL (10, 16). As the accumulation from mildly OxLDL progresses, however, the cholesterol distribution shifts and CE accumulates in the lysosome, suggesting an inhibition of hydrolysis. Importantly, both the OxLDL-derived FC and CE are sequestered in lysosomes and resistant to further cellular metabolism or efflux (17).

The underlying mechanisms that differentiate lipid accumulation after treatment with OxLDL versus AcLDL remain largely unknown. Previous data show that both lipo-

Manuscript received 16 February 2005 and in revised form 17 June 2005.

Published, JLR Papers in Press, July 16, 2005.
DOI 10.1194/jlr.M500059-JLR200

Abbreviations: AcLDL, acetylated low density lipoprotein; AggLDL, aggregated low density lipoprotein; CE, cholesteryl ester; DISP, lipid dispersions; EEA-1, early endosomal antigen-1; EM, electron microscopy; FC, free cholesterol; HMM, human monocyte-derived macrophages; LAMP-1, lysosomal-associated membrane protein-1; OxLDL, oxidized low density lipoprotein; TBARS, thiobarbituric acid-reactive substances; TPA, phorbol ester.

[1] To whom correspondence should be addressed.
e-mail: jay.jerome@vanderbilt.edu

proteins are delivered to the same lysosomes and at similar rates (19), thus ruling this out as an explanation for the differences. Additionally, the buildup of OxLDL-derived CE in lysosomes does not appear to be the result of defective or reduced enzymes, as functional lysosomal acid lipase has been shown in foam cells (13, 20). An effect not observed in AcLDL-treated cells but consistent for mildly OxLDL loading is the accumulation of FC in the lysosome. Thus, this may be a key step in the OxLDL-induced inhibition of hydrolysis. If FC accumulation in lysosomes plays a role in lysosomal dysfunction, then other sources of cholesterol that induce FC buildup in lysosomes should exhibit effects similar to those of OxLDL. Alternative sources of modified cholesterol, such as aggregated low density lipoprotein (AggLDL) or CE-rich lipid dispersions (DISP), have been shown to traffic through lysosomes and result in foam cell genesis (14, 21–24). However, it is unclear how these modifications induce macrophage foam cells. We report here that treatment with AggLDL as well as with DISP mimics the lysosomal accumulation of FC found with OxLDL treatment. Furthermore, the inhibition of hydrolysis observed in OxLDL-treated macrophages is also observed in macrophages treated with AggLDL and DISP. Using biochemical and microscopic analyses, we conclude that alternative sources of cholesterol in addition to OxLDL are capable of inducing lysosomal FC and CE accumulation and may have profound effects on foam cell lipid metabolism.

MATERIALS AND METHODS

Materials

THP-1 human monocytes/macrophages were purchased from ATCC (Manassas, VA). BSA, EDTA, cholesteryl oleate, phosphatidylcholine, phosphatidylserine, cholesteryl methyl ether, Nile red stain, and filipin were purchased from Sigma-Aldrich (St. Louis, MO). FBS was obtained from Hyclone (Logan, UT), and RPMI, L-glutamine, Eagle's vitamins, streptomycin, and penicillin were purchased from Mediatech (Herndon, VA). All tissue culture plasticware was purchased from Corning (Corning, NY). All other chemical reagents and chemical solvents were obtained from VWR (West Chester, PA). The ACAT inhibitor CP113,818 was a generous gift from Pfizer Central Research (Groton, CT). Lysosomal-associated membrane protein-1 (LAMP-1) mouse IgG antibody was purchased from BD Biosciences (San Jose, CA). Early endosomal antigen-1 (EEA-1) rabbit IgG was purchased from Affinity BioReagents (Golden, CA). Rhodamine (TRITC)-conjugated $F(ab)_2$ fragment goat anti-mouse and goat anti-rabbit IgG were obtained from Jackson ImmunoResearch Laboratories, Inc. (West Grove, PA).

Lipoprotein isolation and aggregation

Human LDL was isolated from plasma collected from fasted, normocholesterolemic human volunteers according to procedures approved by the Human Subjects Institutional Review Board. LDL was isolated by sequential ultracentrifugation ($1.006 < d < 1.063$) (17). LDL was dialyzed against 0.9% NaCl containing EDTA (0.3 mmol/l) for 72 h, filter-sterilized through a Millipore filter (0.45 μm), and stored under nitrogen at 4°C. Isolated LDL was aggregated by vortex (1 min) followed by sonication with a Branson sonifier (10 min, 70% duty cycle) on ice to break up large aggregates and passed through a 0.45 μm filter. This produces small (~30–75 nm) aggregates that produce maximal uptake and lysosomal delivery. Aggregation of LDL and size were confirmed by negative staining with 2% phosphotungstic acid. Measurement of thiobarbituric acid-reactive substances (TBARS) and conjugated diene levels confirmed the absence of oxidation after the aggregation procedure.

Preparation of DISP

Anisotropic CE-rich DISP were prepared under sterile conditions, as described by Mahlberg et al. (22). Briefly, cholesteryl oleate (30 mg), phosphatidylcholine (1 mg), and phosphatidylserine (0.1 mg) were combined in a sterile 50 ml Corex glass tube and dried under nitrogen. RPMI medium (17 ml) supplemented with HEPES (12.5 mM) was then added and subjected to a water bath at 80°C for 20 min to melt the dried lipids. The solution was sonicated for 20 min using a Branson sonifier (50% duty cycle). TBARS levels showed no oxidation after sonication of DISP. Dispersion size was confirmed by negative staining with 2% phosphotungstic acid. The loading medium contained 60 μg CE/ml DISP. To ensure contact of cells with dispersions, an inverted cell culture technique was used (22). Cells were plated on glass coverslips on the bottom of 35 mm dishes and then inverted on sterile rings. Loading medium was then added so that the coverslip was submerged.

Cell culture of THP-1 and human macrophages

THP-1 macrophages were plated onto 35 mm wells or coverslips at a density of 1.5×10^6 cells and incubated for 3–4 days at 37°C in RPMI containing 10% FBS and 50 ng/ml phorbol ester (TPA), to allow for differentiation into macrophages. TPA was included in the incubation medium throughout the duration of the experiments. Culture media for all incubations were supplemented with HEPES (20 mmol/l), Eagle's vitamins, L-glutamine (200 mmol/l), streptomycin (100 μg/ml), penicillin (100 IU/ml), and β-mercaptoethanol (0.008 μl/ml). Human monocytes were isolated from whole blood using Histopaque 1.077 (Sigma) density gradients and purified using cell depletion with magnetic beads (Mitenyl Biotec, Auburn, CA). They were differentiated into human monocyte-derived macrophages (HMM) during 6 days of culture in RPMI-1640 medium with 10% human serum. Macrophages were incubated with medium containing 1% fatty acid-free BSA for 24 h before cholesterol loading to minimize excess triglyceride in cells.

Cholesterol loading and analysis

To measure cholesterol loading, macrophages were incubated for 0–6 days at 37°C in culture medium containing 1% FBS alone or with either 100 μg protein/ml AggLDL or AcLDL or 60 μg/ml DISP. In some experiments, the ACAT inhibitor compound CP113,818 (1.5 μg/ml medium) was included in the medium to localize CE accumulation. Comparison of FC and CE in cells with and without ACAT inhibition provided a means of determining whether CE in uninhibited cells was derived from ACAT or was unhydrolyzed lysosomal CE. The cholesterol loading medium was changed every 3–4 days to fresh medium containing the cholesterol loading vehicle.

To quantify cellular cholesterol and determine cholesterol distribution, cellular lipids were extracted by incubation in 2 ml of isopropanol containing 5–10 μg of cholesteryl methyl ether as an internal standard. Dispersion-treated cells were also further extracted after isopropanol incubation with a Bligh and Dyer extraction (25). The lipid extract cholesterol content was then quantified by gas-liquid chromatography according to the procedure of Ishikawa et al. (26) with modification by Klansek et al. (27). Cell proteins were solublized in 1 N NaOH overnight, and protein content was measured using the method of Lowry et al. (28).

To measure the rate of reesterification of cholesterol to CE, we measured the incorporation of [^{3}H]oleate into [^{3}H]CE using methods described previously (29). This involves including a complex of BSA and sodium [^{3}H]oleate in the culture medium during cholesterol loading and measuring the incorporation of radioactivity into the CE band after separation by TLC. In some incubations, the ACAT inhibitor CP113,818 was included in the incubation medium as a control to confirm that any [^{3}H]CE formation was the result of ACAT.

[^{3}H]oleate incorporation into triglycerides as a measure of triglyceride synthesis was also measured by TLC and scintillation counting, as described previously (24). Triglyceride mass in the isopropanol extracts was measured using an assay kit from Boehringer Mannheim. Triglyceride synthesis was minimal during the course of the experiments, consistent with our finding that triglycerides did not accumulate under the incubation conditions we used. The maximum increase in triglyceride mass was in one experiment in which triglycerides increased from 14 to 66 μg/mg cell protein. In other experiments, triglyceride levels remained <40 μg/mg cell protein. No significant ($P < 0.05$) differences in triglyceride were seen between AggLDL and AcLDL loading.

Cell viability during loading was assessed by counts of cell number, protein levels, and adenine release (30). Cell density was determined by counting the number of cells in 15 microscope fields per condition (each field was 40,000 μm^2), determining the average number of cells per square micrometer, and then multiplying by the total area of the dish or coverslip. To determine adenine release, macrophages were incubated with 1.0 μCi of [^{3}H]adenine in medium containing 0.2% BSA for 2 h. This medium was removed, and the monolayers were then equilibrated for 10 min in 0.2% BSA-containing medium. After equilibration, fresh medium was added for 24 h. After this time, 150 μl of medium was removed and filtered (Multiscreen Filtration System; Millipore Corp., Billerica, MA). Aliquots were analyzed for the release of cellular tritium. By all measures, the loss of THP-1 cells during the incubation was <3% for loading via AggLDL or DISP either for 6 days or with 6 days of loading followed by 4 days without lipoprotein. This level of cell death was not statistically different from that for untreated cultures. HMM loaded via AggLDL for 6 days also showed <3% cell death.

Microscopy

After cholesterol loading, microscopy was used to visualize cellular lipids and determine cellular compartmentalization. Fluorescence microscopy visualized neutral lipid by Nile red staining. FC was visualized by filipin staining. Lysosomes/late endosomes and early endosomes were visualized using primary antibodies for LAMP-1 and EEA-1, respectively, followed by a rhodamine (TRITC)-conjugated F(ab)$_2$ fragment goat anti-mouse or goat anti-rabbit IgG secondary antibody. For all light microscopy stainings, cells were plated on coverslips placed on the bottom of 35 mm dishes. After incubations, cells were washed in PBS and fixed for 15 min in 2.5% neutral buffered paraformaldehyde. For Nile red staining, the fixed cells were washed in PBS and then mounted on glass slides with a phenylenediamine-glycerol mounting medium containing Nile red stain (2 μg/ml). For filipin staining, cells were washed in PBS and stained by incubation at room temperature with filipin stain solution (1.25 mg of filipin dissolved in 0.5 ml of dimethyl sulfoxide, diluted in 25 ml of PBS). For LAMP-1 or EEA-1 staining, the cells were washed in PBS, followed by a brief wash in 10% glycine and two 5 min washes in BSP blocking buffer (1% BSA and 0.1% saponin in dPBS). The cells were then incubated in a humid environment at room temperature for 1 h with primary antibody solubilized in BSP buffer. After a thorough wash in BSP buffer, the cells were treated with secondary antibody for 1 h in a similar environment. Incubations with only primary or secondary antibodies were performed simultaneously as controls for the immunostaining procedure. LAMP-1 antibody was used at a concentration of 10 μg/ml, and EEA-1 was used at a concentration of 4 μg/ml. TRITC was used at a concentration of 2.5 μg/ml. In some experiments to localize FC to specific locations, immunostained preparations were costained with filipin using our standard filipin procedure. After staining, immunostained or filipin-stained preparations were washed in PBS and mounted on glass slides with a phenylenediamine-glycerol solution to reduce photobleaching.

Results were evaluated with a Zeiss Axioplan Motorized Fluorescent Microscope (Oberkochen, Germany) equipped with a Photometrics Coolsnap charge-coupled device camera (Nikon Instruments, Melville, NY). Nile red was visualized using a bandpass 475/40 filter for excitation and a bandpass 530/50 filter for emission. These wavelengths are specific for neutral lipid (31). The presence of filipin-positive FC was detected with untraviolet filter excitation and viewed through a 510 nm barrier filter. TRITC was visualized with a 545/30 excitation filter and viewed through a 620/60 bandpass filter. Images were processed with Metamorph (Universal Imaging Co.) and Photoshop (Adobe) software.

Transmission electron microscopy (EM) was performed using a Phillips CM-12 operated at 80 Kiloelectron Volt to ultrastructurally analyze cell lysosomal lipid volume. For the preparation of thin sections, cell monolayers were washed in cacodylate buffer and fixed in 2.5% glutaraldehyde. Lysosomes and related organelles were localized by the presence of acid phosphatase using a modification of the Gomori lead precipitation method (32). β-Glycerol phosphate was used as a substrate, and the reaction control was incubated in identical medium not containing the enzymatic substrate. After incubation, cells were postfixed in 1% osmium tetroxide, dehydrated, and embedded in epoxy resin. Before further staining, the sections were viewed to verify the enzymatic reaction and then stained with uranyl acetate.

Statistics

All data are expressed as means ± SD of triplicate measures. Data were graphed and statistical analysis performed using Student's *t*-test. Arcsine transformation was performed before *t*-test for percentages. The criterion for significance was set at $P < 0.05$ for a type I error.

RESULTS

Incubation of THP-1 human macrophages with AggLDL produced significant FC and CE accumulation, similar to our previous experiments with mildly OxLDL. **Figure 1** shows the results from a representative experiment. THP-1 cells treated with 100 μg/ml AggLDL resulted in a continuous increase in total cellular cholesterol, reaching excesses of 250 μg/mg cell protein by day 6 (Fig. 1). This is considered to be in the range of foam cell concentrations. After 2 days of incubation, 46.4% of the total cholesterol was unesterified. However, as cholesterol accumulation continued, the rate of FC accumulation was reduced and mostly CE accumulated. At day 6, only 30.4% of cholesterol was FC. Human monocyte-derived macrophages incubated with 100 μg/ml AggLDL showed a similar accumulation and distribution pattern. At day 2, cells had an average of 168 ± 42 μg cholesterol/mg cell protein. Thirty-

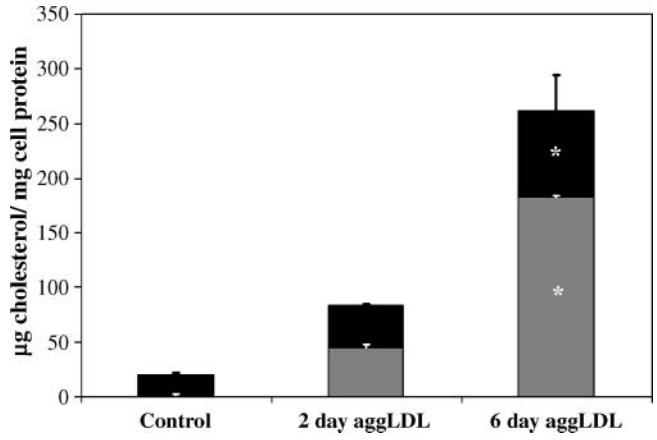

Fig. 1. Accumulation of free cholesterol (FC; black bars) and cholesteryl ester (CE; gray bars) in THP-1 macrophages incubated with aggregated low density lipoprotein (AggLDL). THP-1 macrophages were treated for 2 or 6 days at 37°C in RPMI containing 1% FBS and phorbol ester (TPA; 50 ng/ml) alone or with 100 µg protein/ml AggLDL. The cells were harvested and cell cholesterol content was analyzed by gas-liquid chromatography as described in Materials and Methods. Values are means ± SD for triplicate dishes. * $P < 0.05$ versus day 2.

eight percent of this was unesterified. HMM at day 6 averaged 322 ± 23 µg cholesterol/mg cell protein, with only 23% of this as FC.

Because EM of both THP-1 and HMM showed that lysosomal volume continued to increase (data not shown), this significant reduction in FC percentage by day 6 ($P < 0.005$) suggests an inhibition of CE hydrolysis as a result of AggLDL treatment. Ultrastructure observation showed that most of the lipid in cells incubated for 6 days with AggLDL accumulated within lysosomes (**Fig. 2**). Nile red staining

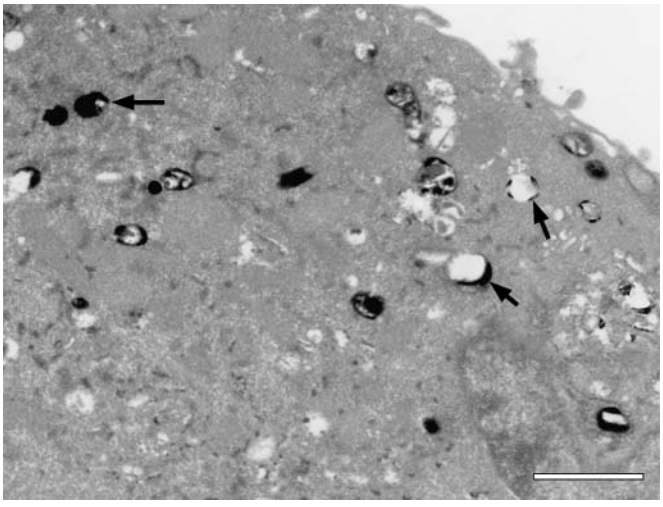

Fig. 2. Electron micrograph of cellular lipid accumulation in THP-1 macrophages incubated with 100 µg protein/ml AggLDL for 6 days. The cholesterol-enriched cells display lipid-filled lysosomes, as indicated by the presence of dark, acid phosphatase reaction product (arrows). Cells are unstained except for the acid phosphatase reaction and osmium postfixation. Magnification = 4,000×; bar = 2 µm.

confirmed that neutral lipid accumulated in AggLDL-treated THP-1 cells (**Fig. 3A**, **E**) in a distribution corresponding to the lysosomal lipid seen with EM. We used filipin staining to determine whether FC accumulated in lysosomes. At day 2 of AggLDL incubation, the majority of FC accumulation from AggLDL colocalized with LAMP-1 (Fig. 3B–D). After 6 days of incubation with AggLDL, more FC staining was observed (Fig. 3F), a portion of which colocalized in vesicles in which the membranes stained positive for LAMP-1 (Fig. 3G, H). FC deposits did not colocalize with a marker for early endosomes at either 2 or 6 days (data not shown). Comparison of filipin, Nile red, and LAMP-1 stainings with biochemical measures of cholesterol mass suggested that after 6 days the lysosome content consisted mainly of CE with a smaller portion of FC. Human monocyte-derived macrophages showed a similar FC deposit in LAMP-1-positive vesicles, and EM confirmed that most (>70%) of the lipid accumulation from AggLDL was in lysosomes.

As stated above, lysosomal accumulation of FC was verified by filipin staining. To confirm that CE also accumulated within lysosomes, we compared THP-1 cells loaded in the absence or presence of CP113,818. If the accumulated CE was unhydrolyzed CE, then ACAT inhibition should produce little change in the CE/FC ratio. On the other hand, if the CE in cells was the result of extralysosomal ACAT-driven FC reesterification, then ACAT inhibition should increase FC levels and decrease CE concentrations. **Figure 4A** shows results from a representative experiment of cholesterol accumulation in AggLDL-treated cells in the presence of CP113,818. The ACAT inhibition experiments were run in parallel and under the same conditions to those illustrated in Fig. 1. When the percentages of FC versus CE in Fig. 4A are compared with data from Fig. 1, ACAT-inhibited THP-1 cells after 2 days of cholesterol enrichment showed a significant increase (26.90%) in cellular FC content from noninhibited cells ($P < 0.005$) (Fig. 4B). This indicates that some but not all of the CE in cells at day 2 was derived from ACAT. By day 6, however, FC increased by only 9.81% when ACAT was inhibited. Thus, by day 6, most of the CE in the cells was unhydrolyzed lipoprotein CE trapped within lysosomes. To confirm that cellular cholesterol was not available for reesterification, we repeated the loading experiments with AggLDL in the presence of [^{3}H]oleate and measured its incorporation into CE on days 1 and 3. Cells treated with AggLDL showed 19 nm [^{3}H]oleate incorporation into cellular CE. In comparison, AcLDL-treated cells incorporated 39 nm [^{3}H]oleate into cellular CE. At day 3, the incorporation into cellular CE had decreased to 9 nm for AggLDL-treated cells but continued to increase to 45 nm with AcLDL treatment.

Another naturally occurring modification of lipid capable of generating macrophage foam cells is the lipid particle (5, 7). We have mimicked these particles with CE-rich artificial DISP. These have been shown previously to promote cholesterol loading within cultured macrophages and smooth muscle cells (22, 23, 33). THP-1 macrophages treated for 2 and 6 days with DISP resulted in significant cholesterol accumulation (**Fig. 5**). Even by day 2, total cho-

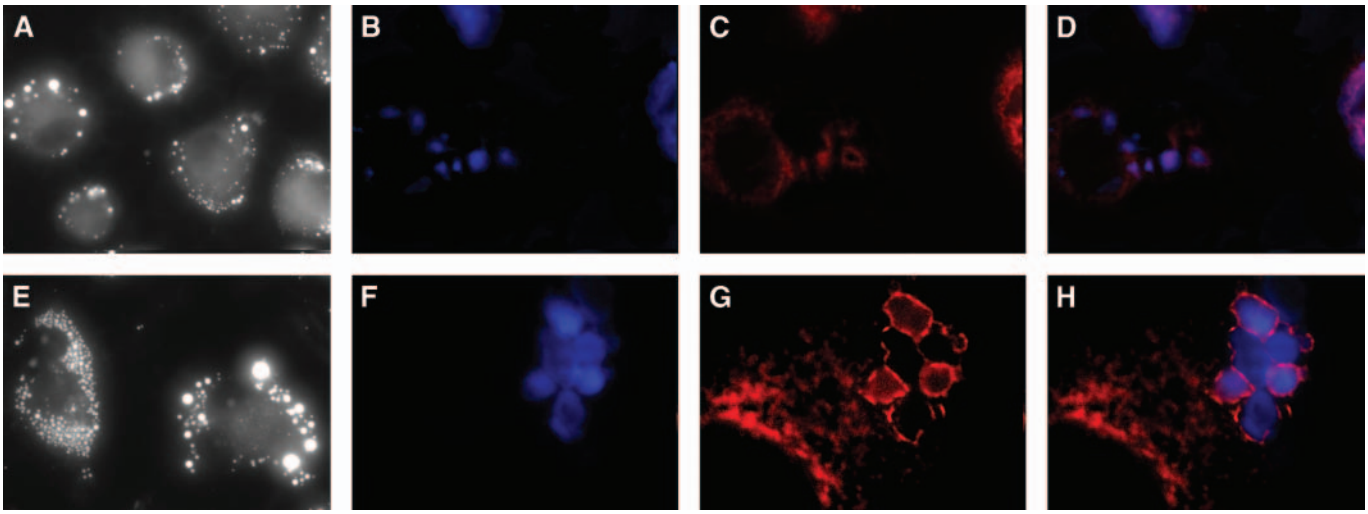

Fig. 3. Localization of neutral lipid, FC, and lysosomal-associated membrane protein-1 (LAMP-1) in THP-1 macrophages after incubation with 100 μg protein/ml AggLDL for 2 (A–D) or 6 (E–H) days. After treatment, cells were fixed and stained as described in Materials and Methods. A, E: Nile red staining shows neutral lipid accumulation by day 2 (A) and further increases in neutral lipid accumulation at day 6 (E). B, F: Punctate areas of filipin staining indicate significant FC accumulation on days 2 and 6. C, G: Large LAMP-1-positive lysosomes were seen on days 2 and 6. D, H: Colocalization of filipin and LAMP-1 staining confirms FC accumulation in lysosomes. Magnification = 200× (A, E), 480× (B–D), and 740× (F–H).

lesterol content reached foam cell concentrations, the majority of which existed as esterified cholesterol. As DISP enrichment continued to day 6, the distribution pattern did not change significantly from day 2 ($P < 0.005$). Additionally, in the presence of CP113,118, the CE/FC ratio was not significantly different from that of uninhibited cells at either time point. Thus, although DISP produced a more rapid accumulation in lysosomes (consisting predominantly of CE), the end point was similar to that seen with AggLDL. In some experiments with DISP, in which loading occurred more slowly, an initial FC accumulation was observed. Overall, though, DISP loaded faster than AggLDL and hydrolysis inhibition occurred sooner.

Visualizing cellular lipid accumulation from DISP by fluorescence microscopy confirmed a lysosomal accumulation (**Fig. 6**). Figure 6A shows Nile red staining of large neutral droplets after 2 days of DISP treatment. The cellular lipid content increased as accumulation continued for 6 days (Fig. 6E). As with AggLDL, significant FC accumulation occurred within LAMP-1-positive lysosomes on days 2 and 6 (Fig. 6B–D, F–H). DISP-induced lysosomal cholesterol accumulation was confirmed by acid phosphatase staining of EM samples in **Fig. 7**. Thus, treatment with DISP seems to induce a rapid influx of cholesterol that traffics to the lysosome and results in extensive CE accumulation similar to that seen with prolonged AggLDL treatment.

DISCUSSION

Much of our knowledge of foam cell cholesterol metabolism encompasses research involving AcLDL and OxLDL. Although both modifications are capable of inducing foam cell production, only OxLDL has been physiologically indicated in atherosclerotic lesions, particularly the foam cell-rich areas (34, 35). Oxidation is a modification that produces lysosomal accumulation, an occurrence that is a characteristic of atherosclerotic lesions (10). Thus, the study of OxLDL-induced lipid accumulation is both physiologically relevant and a useful method of furthering our understanding of lysosomal cholesterol sequestration in atherosclerotic lesions.

OxLDL, however, is not the only naturally occurring modification capable of producing macrophage foam cells. Aggregates of LDL have also been found to produce foam cells both in vitro and in vivo (5, 7). Aggregation can occur via a variety of processes, including oxidation, interaction with phospholipase A_2 and C, sphingomyelinase, glycosylation, interactions with extracellular matrix, and mechanical processes (5, 36–44). These various aggregation methods all result in different manipulations of the LDL molecule with varying sizes and molecular arrangement. Some types of aggregates are taken up in macrophages by phagocytosis, but other mechanisms of uptake have also been reported (3, 5, 36, 37). Smaller aggregates (<0.1 μm) have been found to stimulate pinocytotic uptake (44). Very large aggregates can be internalized through engulfment into surface-connected compartments, a process designated "patocytosis" by Kruth and colleagues (45). Patocytosis results in a labyrinth of surface invaginations, resulting in stacks of interdigitated cytoplasmic membrane folds visible by EM (45, 46). In studies by Haberland and colleagues (46), aggregates produced by vortexing or by phospholipase C treatment accumulated within membrane-bound intracellular structures in cultured macrophages. Many of these had a size and intracellular location consistent with the lysosomes we have identified in this study. Moreover, similar lipid-filled structures were found in foam cells within rabbit lesions. The aggregates used in the present study were vortexed briefly, followed by sonication

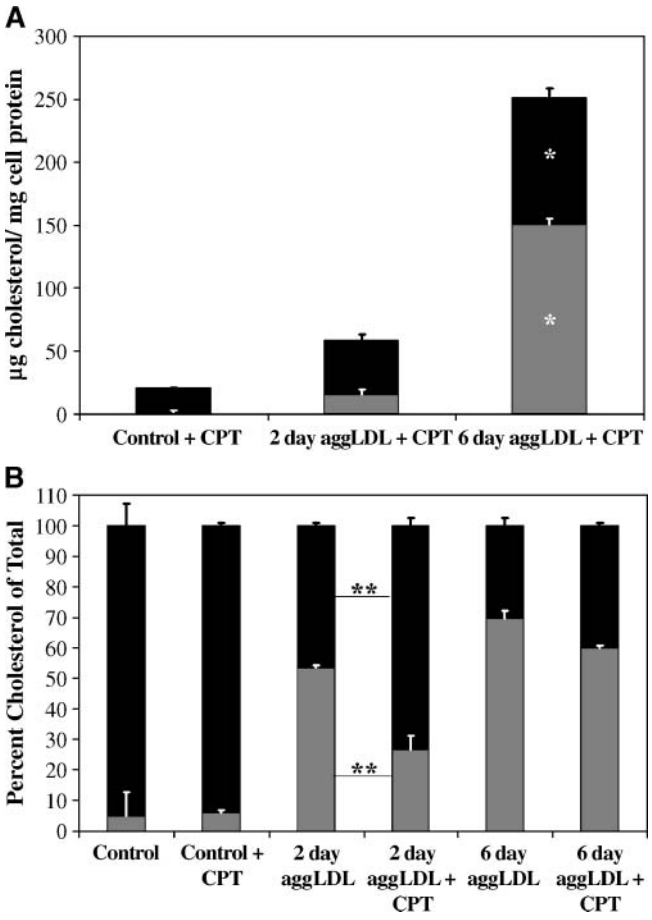

Fig. 4. A: Accumulation of FC (black bars) and CE (gray bars) in THP-1 macrophages incubated with 100 µg protein/ml AggLDL for 2 or 6 days in the presence of 1.5 µg/ml of an ACAT inhibitor, CP113,818. Cellular FC and CE mass after CP113,818 treatment (CPT) were analyzed by gas-liquid chromatography as described in Materials and Methods. Values are means ± SD for triplicate dishes. * $P < 0.05$ versus day 2. B: The percentage change in FC and CE as a result of ACAT inhibition (CPT) determined by comparing values for those cells loaded in the presence of the ACAT inhibitor (A) with similarly treated cells in which ACAT was not inhibited (see Fig. 1). Values are means ± SD for triplicate dishes. ** $P < 0.05$ for CPT-treated versus nontreated cells.

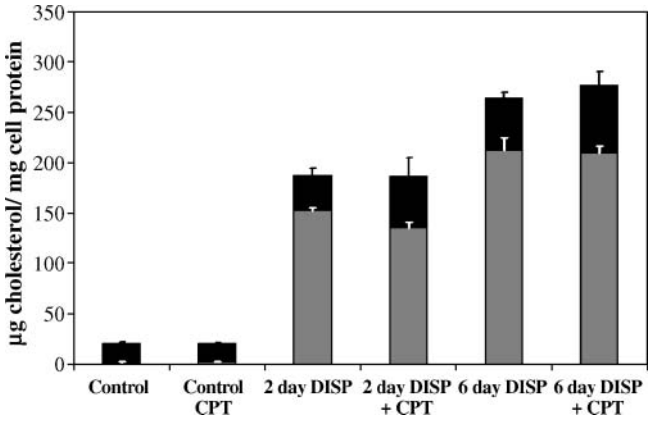

Fig. 5. Accumulation of FC (black bars) and CE (gray bars) in THP-1 macrophages incubated with lipid dispersions (DISP) using the inverted cell culture technique as described in Materials and Methods. THP-1 macrophages were incubated for 2 or 6 days in RPMI containing 1% FBS and TPA (50 ng/mg) alone or with 60 µg CE/ml DISP. The effect of treatment with the ACAT inhibitor CP113,818 (CPT; 1.5 µg/ml) was also analyzed. The cells were harvested and the cellular cholesterol content was analyzed by gas-liquid chromatography as described in Materials and Methods. Values are means ± SD for triplicate dishes. Differences between CPT-treated and non-CPT-treated cells were not significant at $P < 0.05$.

and filtration, resulting in aggregates too large to undergo pinocytosis but too small and arranged differently enough not to participate in patocytosis. Additionally, electron micrographs did not indicate the patocytotic membrane folds described by Kruth et al. (45). Thus, our aggregates most likely undergo receptor-mediated phagocytosis, a pathway that delivers the particles to lysosomes for degradation.

Previous research on AggLDL-enriched macrophages has examined the possible mechanisms of aggregation as well as methods of cellular uptake, but intracellular trafficking of AggLDL remains largely unknown. AggLDL in this study resulted in substantial sequestration of lysosomal lipid, verified by both fluorescence microscopy and EM. Additionally, AggLDL treatment produced an initial lysosomal accumulation of FC, a small portion of which was able to be reesterified by ACAT into cytoplasmic CE inclusions. As FC accumulation continued, however, hydrolyzed FC became increasingly trapped within lysosomes and unavailable to ACAT. At this point, the cholesterol distribution shifted to include increased amounts of unhydrolyzed CE in lysosomes. This pattern of cholesterol accumulation is shared by cells treated with mildly OxLDL (19, 29). Lysosomal accumulation of CE has also been reported for AggLDL formed by complexing with extracellular matrix components such as fibronectin or proteoglycans, although in these studies it was not clear whether the inhibition of hydrolysis was immediate or delayed (21, 47, 48).

Although potent, modified LDL is not the only mechanism of generating cholesterol accumulation in macrophage foam cells. Within atherosclerotic lesions, the extracellular environment contains matrix components, cell remnants, and various complexes of lipid particles (4, 7). Additionally, macrophage foam cells lysed within atherosclerotic lesions can release inclusions that can subsequently undergo uptake by neighboring macrophages and smooth muscle cells (49). CE-rich DISP of similar composition to those found within lesions have been found to induce cholesterol loading in macrophages and smooth muscle cells, the majority of which was found in lipid-filled lysosomes (49). Thus, lipid particles may also be relevant to atherosclerotic lesion development. In this present study, cholesterol accumulation and distribution were examined in macrophages incubated with artificial CE-rich DISP. DISP enrichment produced a similar, but more rapid, increase in cellular cholesterol compared with AggLDL. The cholesterol distribution after DISP treatment resulted in significant lysosomal CE accumulation. The lysosomal character of CE accumulation was confirmed by EM and light microscopy in conjunction with biochemical measures in

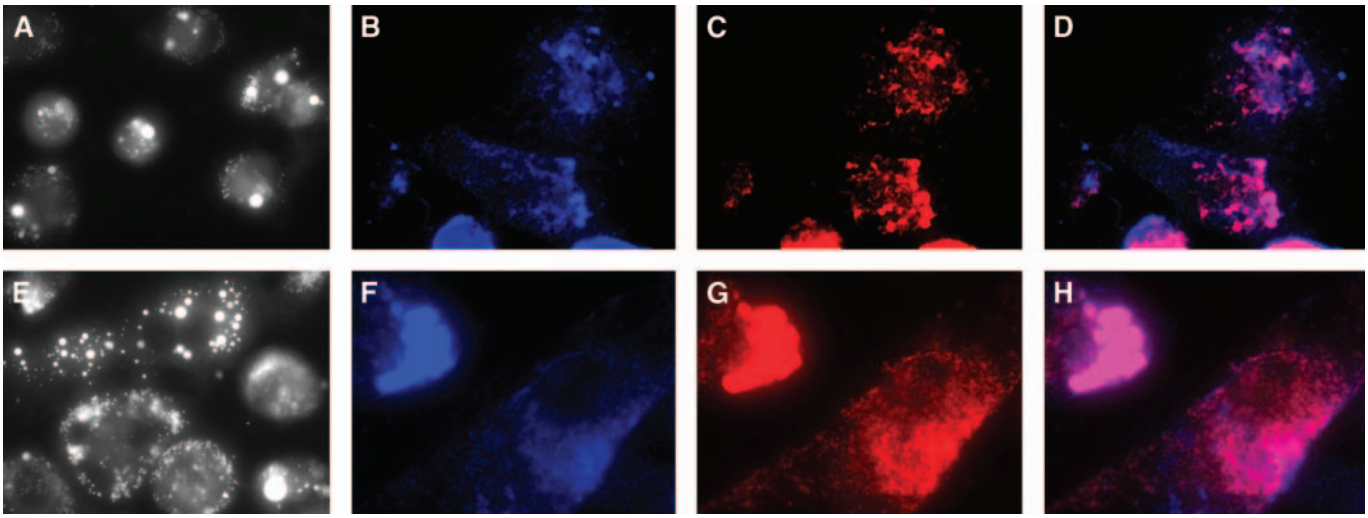

Fig. 6. Localization of neutral lipid, FC, and LAMP-1 in THP-1 macrophages after incubation with 60 μg CE/ml DISP for 2 (A–D) or 6 (E–H) days. After treatment, cells were fixed and stained as described in Materials and Methods. A, E: Nile red staining shows a rapid neutral lipid accumulation by day 2 (A) and increased neutral lipid accumulation at day 6 (E). B, F: Filipin staining of FC after treatment shows areas of FC accumulation on days 2 and 6. C, G: LAMP-1-positive lysosomes could be identified on days 2 and 6. D, H: Colocalization of filipin and LAMP-1 staining confirms FC accumulation within lysosomes. Magnification = 200× (A, E), 320× (B–D), and 400× (E–H).

the presence and absence of an ACAT inhibitor. One possible mechanism behind the faster CE accumulation may be a more rapid processing of droplets and subsequently a more rapid inhibition of lysosomal hydrolysis. Previous studies using similar CE-rich dispersions in J774 murine macrophages reported a rapid uptake of DISP (22). The influx was attributable to efficient utilization of the droplets rather than a saturation of uptake. This study, as well as later studies from the same laboratory (33), describe DISP as undergoing phagocytotic uptake and subsequent FC accumulation in lysosomes. The discrepancy between the FC accumulation in these studies and the CE accumulation seen here may be the result of shorter incubation times (1–3 h in the earlier studies) as well as the use of mouse cells. Mouse macrophages metabolize cholesterol more efficiently than do human macrophages (29).

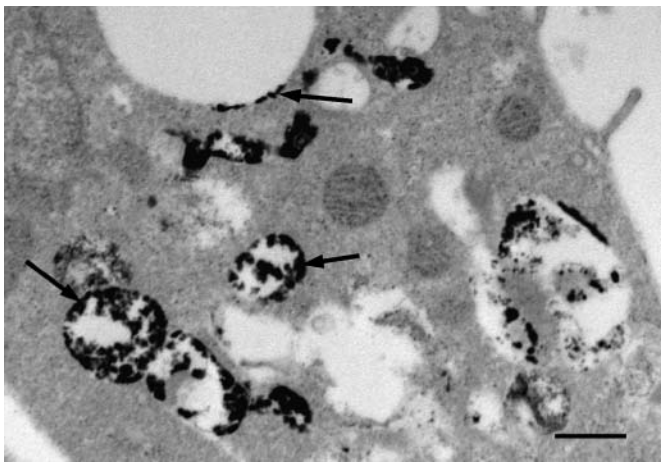

Fig. 7. Electron micrograph of cellular lipid accumulation in THP-1 macrophages treated with DISP. Cells incubated for 6 days with 60 μg CE/ml DISP, as described in Materials and Methods, resulted in extensive lipid accumulation in lysosomes. Lysosomes are confirmed by the presence of dark, acid phosphatase reaction product (arrows). Magnification = 14,000×; bar = 0.5 μm.

The rate of lysosomal cholesterol accumulation may also partly explain the more rapid inhibition of lysosomal hydrolysis by DISP compared with AggLDL. Tabas et al. (50) have reported that LDL and β-VLDL are delivered to distinct endocytotic vesicles, resulting in slower degradation of β-VLDL. Thus, the efficiency of trafficking definitely affects metabolism. A study of the early accumulation of cholesterol from aggregates formed by phospholipase C modification of LDL showed an initial incorporation of radiolabeled oleate into cellular CE, suggesting that the CEs in these aggregates were efficiently hydrolyzed in lysosomes (51). However, incorporation into CEs slowed after 10 h and remained sluggish for the remaining 20 h of their experiment. This is consistent with our observations that lysosomal inhibition took longer than 24 h when AggLDL was the loading vehicle. This suggests that the rate of accumulation of some products of lysosomal processing may influence the timing by which hydrolysis is inhibited.

Despite the small differences, enrichment of human macrophages with AggLDL as well as CE-rich DISP induced foam cell formation in which lysosomal accumulation predominated. The CE/FC ratios seen with AggLDL and DISP are similar to those demonstrated in cells treated with mildly OxLDL (17, 29). Several studies demonstrate that oxidation of LDL leads to lysosomal accumulation, but the mechanism of lysosomal accumulation may vary between different types of OxLDL particles. Although heavily OxLDL seems to directly inhibit CE hydrolysis by various means (15, 18, 52–54), our previous studies indicate a more indirect mechanism for mildly OxLDL (29). Importantly, the accumulation of FC and CE from mildly OxLDL is similar

to that seen in atherosclerotic lesions. In the present study, our aggregates of LDL as well as DISP showed no evidence of oxidation yet resulted in similar cholesterol accumulation. Therefore, this study indicates that inhibition of CE hydrolysis is not dependent on oxidized lipids. Furthermore, the inhibition of hydrolysis is not immediate, particularly with AggLDL. This further suggests an indirect rather than a direct inhibition of CE hydrolysis.

A common link between AggLDL, DISP, and mildly OxLDL may be, at least in part, an initial accumulation of FC in lysosomes. An initial accumulation of FC was seen in this study and has been reported in other studies demonstrating lysosomal lipid accumulation (17, 51, 55, 56). Given the FC-induced effects on membrane fluidity and membrane protein function (57–59), it is reasonable to hypothesize that increases in FC may interfere with normal lysosomal function and thus interrupt hydrolysis. Possible cholesterol-mediated processes could include disturbance of the lysosomal environment or disruption of the trafficking of lysosomal hydrolases. Thus, elucidation of FC accumulation-induced effects on lysosomal function may provide insight into foam cell lipid metabolism. However, whatever the mechanism, lysosomal accumulation is not a universal feature of all cellular lipoprotein metabolism, because it does not occur with AcLDL treatment.

We have shown here that multiple sources of cholesterol can induce foam cells with lysosomal cholesterol accumulation similar to that seen in atherosclerotic lesions. This suggests that in vivo, multiple sources of cholesterol may also be involved in foam cell genesis. In AggLDL-, DISP-, and mildly OxLDL-treated macrophages, lysosomal hydrolysis is eventually disrupted. Because this effect is not dependent on oxidation, lysosomal dysfunction may occur by general rather than specific mechanisms. This observation indicates that other lysosomal functions may also be interrupted in foam cells, which could have profound effects on foam cell metabolism and atherosclerosis progression, and suggests that an acquired lysosomal defect is one of the multiple factors influencing atherogenesis.

This work was supported by Grant 2 RO1 HL-49148-04A2 from the National Institutes of Health, National Heart, Lung, and Blood Institute. EM was carried out in the Vanderbilt Research Electron Microscopy Core of the Cell Imaging Shared Resource, supported by National Institutes of Health Grants DK-20539, CA-68485, and DK-58404.

REFERENCES

1. Brown, M. S., and J. L. Goldstein. 1983. Lipoprotein metabolism in the macrophage. *Annu. Rev. Biochem.* **52:** 223–261.
2. Aviram, M. 1993. Modified forms of low density lipoprotein and atherosclerosis. *Atherosclerosis.* **98:** 1–9.
3. Khoo, J. C., E. Miller, P. McLoughlin, and D. Steinberg. 1988. Enhanced macrophage uptake of low density lipoprotein after self-aggregation. *Arteriosclerosis.* **8:** 348–358.
4. Chao, F-F., E. Blanchette-Mackie, Y-J. Chen, B. Dickens, E. Berlin, L. Amende, S. Skarlatos, W. Gamble, J. Resau, W. Mergner, et al. 1990. Characterization of two unique cholesterol-rich lipid particles isolated from human atherosclerotic lesions. *Am. J. Pathol.* **136:** 169–179.
5. Kruth, H. 2002. Sequestration of aggregated low-density lipoproteins by macrophages. *Curr. Opin. Lipidol.* **13:** 483–488.
6. Brown, A., E. Mander, I. Gelissen, L. Kritharides, R. Dean, and W. Jessup. 2000. Cholesterol and oxysterol metabolism and subcellular distribution in macrophage foam cells: accumulation of oxidized esters in lysosomes. *J. Lipid Res.* **41:** 226–236.
7. Guyton, J., and K. Klemp. 1988. Ultrastructural discrimination of lipid droplets and vesicles in atherosclerosis: value of osmium-thiocarbohydrazide-osmium and tannic acid-paraphenylenediamine techniques. *J. Histochem. Cytochem.* **36:** 1319–1328.
8. Werb, Z., and Z. A. Cohn. 1972. Cholesterol metabolism in the macrophage. III. Ingestion and intracellular fate of cholesterol and cholesterol esters. *J. Exp. Med.* **135:** 21–44.
9. Brown, M. S., Y. K. Ho, and J. L. Goldstein. 1980. The cholesteryl ester cycle in macrophage foam cells. Continual hydrolysis and re-esterification of cytoplasmic cholesteryl ester. *J. Biol. Chem.* **255:** 9344–9352.
10. Jerome, W. G., and J. C. Lewis. 1985. Early atherogenesis in White Carneau pigeons. II. Ultrastructural and cytochemical observations. *Am. J. Pathol.* **119:** 210–222.
11. Fowler, S., P. Berberian, H. Shio, S. Goldfischer, and H. Wolinsky. 1980. Characterization of cell populations isolated from aortas of rhesus monkeys with experimental atherosclerosis. *Circ. Res.* **46:** 520–530.
12. deDuve, C. 1974. The participation of lysosomes in the transformation of smooth muscle cells to foamy cells in the aorta of cholesterol fed rabbits. *Acta Cardiol. Suppl.* **20:** 9–25.
13. Haley, N., S. D. Fowler, and C. deDuve. 1980. Lysosomal acid cholesteryl esterase activity in normal and lipid-laden aortic cells. *J. Lipid Res.* **21:** 961–969.
14. Dhaliwal, B., and U. Steinbrecher. 2000. Cholesterol delivered to macrophages by oxidized low density lipoprotein is sequestered in lysosomes and fails to efflux normally. *J. Lipid Res.* **41:** 1658–1665.
15. Lougheed, M., H. Zhang, and U. Steinbrecher. 1991. Oxidized low density lipoprotein is resistant to cathepsins and accumulates within macrophages. *J. Biol. Chem.* **266:** 14519–14525.
16. Jerome, W., C. Cash, R. Webber, R. Horton, and P. Yancey. 1998. Lysosomal lipid accumulation from oxidized low density lipoprotein is correlated with hypertrophy of the Golgi apparatus and trans-Golgi network. *J. Lipid Res.* **39:** 1362–1371.
17. Yancey, P. G., and W. G. Jerome. 2001. Lysosomal cholesterol derived from mildly oxidized low density lipoprotein is resistant to efflux. *J. Lipid Res.* **42:** 317–327.
18. Jessup, W., E. L. Mander, and R. T. Dean. 1992. The intracellular storage and turnover of apolipoprotein B of oxidized LDL in macrophages. *Biochim. Biophys. Acta.* **1126:** 167–177.
19. Yancey, P. G., S. Miles, J. Schwegel, and W. G. Jerome. 2002. Uptake and trafficking of mildly oxidized LDL and acetylated LDL in THP-1 cells does not explain the differences in lysosomal metabolism of these two lipoproteins. *Microsc. Microanal.* **8:** 81–93.
20. Fowler, S., and W. Brown. 1984. Lysosomal acid lipase. *In* Lipases. B. Borgstrom and H. Brockman, editors. Elsevier Biomedical Press, Amsterdam. 329–364.
21. Salisbury, B., D. Falcone, and C. Minick. 1985. Insoluble low density lipoprotein-proteoglycan complexes enhance cholesteryl ester accumulation in macrophages. *Am. J. Pathol.* **120:** 6–11.
22. Mahlberg, F., J. M. Glick, W. G. Jerome, and G. H. Rothblat. 1990. Metabolism of cholesteryl ester lipid droplets in a J774 macrophage foam cell model. *Biochim. Biophys. Acta.* **1045:** 291–298.
23. Minor, L. K., F. H. Mahlberg, W. G. Jerome, J. C. Lewis, G. H. Rothblat, and J. M. Glick. 1991. Lysosomal hydrolysis of lipids in a cell culture model of smooth muscle foam cells. *Exp. Mol. Pathol.* **54:** 159–171.
24. Avart, S., D. Bernard, W. Jerome, and J. Glick. 1999. Cholesteryl ester hydrolysis in J774 macrophages occurs in the cytoplasm and lysosomes. *J. Lipid Res.* **40:** 405–414.
25. Bligh, E. G., and W. J. Dyer. 1959. A rapid method for total lipid extraction and purification. *Can. J. Biochem. Physiol.* **37:** 911–917.
26. Ishikawa, T. T., J. MacGee, J. A. Morrison, and C. J. Glueck. 1974. Quantitative analysis of cholesterol in 5 to 20 μl of plasma. *J. Lipid Res.* **15:** 286–291.
27. Klansek, J. J., P. G. Yancey, R. W. St. Clair, R. T. Fischer, W. J. Johnson, and J. M. Glick. 1995. Cholesterol quantitation by GLC: artifactual formation of short-chain steryl esters. *J. Lipid Res.* **36:** 2261–2266.
28. Lowry, O. H., N. J. Rosebrough, A. L. Farr, and R. J. Randall. 1951. Protein measurement with the Folin phenol reagent. *J. Biol. Chem.* **193:** 265–275.

29. Yancey, P. G., and W. G. Jerome. 1998. Lysosomal sequestration of free and esterified cholesterol from oxidized low density lipoprotein in macrophages of different species. *J. Lipid Res.* **39:** 1349–1361.
30. Shirhatti, V., and G. Krishna. 1985. A simple and sensitive method for monitoring drug-induced cell injury in cultured cells. *Anal. Biochem.* **147:** 410–418.
31. Greenspan, P., and S. Fowler. 1985. Spectrofluorometric studies of the lipid probe, Nile red. *J. Lipid Res.* **26:** 781–789.
32. Gomori, G. 1950. An improved histochemical technic for acid phosphatase. *Stain Technol.* **25:** 81–85.
33. Tangirala, R. K., F. H. Mahlberg, J. M. Glick, W. G. Jerome, and G. H. Rothblat. 1993. Lysosomal accumulation of unesterified cholesterol in model macrophage foam cells. *J. Biol. Chem.* **268:** 9653–9660.
34. Yla-Herttuala, S., W. Palinski, M. Rosenfeld, S. Parthasarathy, T. Carew, S. Butler, J. Witztum, and D. Steinberg. 1989. Evidence for the presence of oxidatively modified low density lipoprotein in atherosclerotic lesions of rabbit and man. *J. Clin. Invest.* **84:** 1086–1095.
35. Rosenfeld, M. E., J. C. Khoo, E. Miller, S. Parthasarathy, W. Palinski, and J. L. Witztum. 1991. Macrophage-derived foam cells freshly isolated from rabbit atherosclerotic lesions degrade modified lipoproteins, promote oxidation of low-density lipoproteins, and contain oxidation-specific lipid-protein adducts. *J. Clin. Invest.* **87:** 90–99.
36. Suits, A. G., A. Chait, M. Aviram, and J. W. Heinecke. 1989. Phagocytosis of aggregated lipoprotein by macrophages: low density lipoprotein receptor-dependent foam cell formation. *Proc. Natl. Acad. Sci. USA.* **86:** 2713–2717.
37. Tertov, V., I. Sobenin, Z. Gabbosov, E. Popov, A. Yaroslavov, M. Jauhiainen, C. Ehnholm, V. Smirnov, and A. Orekhov. 1992. Three types of naturally occurring modified lipoproteins induce intracellular lipid accumulation in human aortic intimal cells. The role of lipoprotein aggregation. *Eur. J. Clin. Chem. Biochem.* **30:** 171–178.
38. Hoff, H., J. O'Neil, J. Pepin, and T. Cole. 1990. Macrophage uptake of cholesterol-containing particles derived from LDL and isolated from atherosclerotic lesions. *Eur. Heart J.* **11 (Suppl. E):** 105–115.
39. Xu, S., and B. Lin. 2001. The mechanism of oxidation-induced low-density lipoprotein aggregation: an analogy to colloidal aggregation and beyond. *Biophys. J.* **81:** 2403–2413.
40. Maor, I., and M. Aviram. 1994. Oxidized low density lipoprotein leads to macrophage accumulation of unesterified cholesterol as a result of lysosomal trapping of the lipoprotein hydrolyzed cholesteryl ester. *J. Lipid Res.* **35:** 803–819.
41. Maor, I., and M. Aviram. 1999. Macrophage-released proteoglycans are involved in cell-mediated aggregation of LDL. *Atherosclerosis.* **142:** 57–66.
42. Falcone, D., and B. Salisbury. 1988. Fibronectin stimulates macrophage uptake of low-density lipoprotein-heparin-collagen complexes. *Arteriosclerosis.* **8:** 263–273.
43. Steinberg, D., S. Parthasarathy, T. Carew, J. Khoo, and J. Witztum. 1989. Beyond cholesterol. modification of low-density lipoproteins that increase its atherogenicity. *N. Engl. J. Med.* **320:** 915–924.
44. Xu, X. X., and I. Tabas. 1991. Sphingomyelinase enhances low density lipoprotein uptake and ability to induce cholesteryl ester accumulation in macrophages. *J. Biol. Chem.* **266:** 24849–24858.
45. Kruth, H., J. Chang, I. Ifrim, and W-Y. Zhang. 1999. Characterization of patocytosis: endocytosis into macrophage surface-connected compartments. *Eur. J. Cell Biol.* **78:** 91–99.
46. Haberland, M., G. Mottino, M. Le, and J. Frank. 2001. Sequestration of aggregated LDL by macrophages studied with freeze-etch electron microscopy. *J. Lipid Res.* **42:** 605–619.
47. Falcone, D., N. Mated, H. Shio, C. Minick, and S. Fowler. 1984. Lipoprotein-heparin-fibronectin-denatured collagen complexes enhance cholesteryl ester accumulation in macrophages. *J. Cell Biol.* **99:** 1266–1274.
48. Vijayagopal, P., S. Srinivasan, K. Jones, B. Radhakrishnamurthy, and G. Berenson. 1985. Complexes of low-density lipoproteins and arterial proteoglycan aggregates promote cholesteryl ester accumulation in mouse macrophages. *Biochim. Biophys. Acta.* **837:** 252–261.
49. Wolfbauer, G., J. M. Glick, L. K. Minor, and G. H. Rothblat. 1986. Development of the smooth muscle foam cell: uptake of macrophage lipid inclusions. *Proc. Natl. Acad. Sci. USA.* **83:** 7760–7764.
50. Tabas, I., S. Lim, X. X. Xu, and F. R. Maxfield. 1990. Endocytosed b-VLDL and LDL are delivered to different intracellular vesicles in mouse peritoneal macrophages. *J. Cell Biol.* **111:** 929–940.
51. Heinecke, J., A. Suits, M. Aviram, and A. Chait. 1991. Phagocytosis of lipase-aggregated low density lipoprotein promotes macrophage foam cell formation: sequential morphological and biochemical events. *Arterioscler. Thromb.* **11:** 1643–1651.
52. Hoppe, G., J. O'Neil, and H. F. Hoff. 1994. Inactivation of lysosomal proteases by oxidized low density lipoprotein is partially responsible for its poor degradation by mouse peritoneal macrophages. *J. Clin. Invest.* **94:** 1506–1512.
53. Roma, P., F. Bernini, R. Fogliatto, S. M. Bertulli, S. Negri, R. Fumagalli, and A. L. Catapano. 1992. Defective catabolism of oxidized LDL by J774 murine macrophages. *J. Lipid Res.* **33:** 819–829.
54. Kritharides, L., W. Jessup, E. L. Mander, and R. T. Dean. 1995. Apolipoprotein A-I-mediated efflux of sterols from oxidized LDL-loaded macrophages. *Arterioscler. Thromb. Vasc. Biol.* **15:** 276–289.
55. Maor, I., H. Mandel, and M. Aviram. 1995. Macrophage uptake of oxidized LDL inhibits lysosomal sphingomyelinase, thus causing the accumulation of unesterified cholesterol-sphingomyelin-rich particles in the lysosomes. A possible role for 7-ketocholesterol. *Arterioscler. Thromb. Vasc. Biol.* **15:** 1378–1387.
56. Roma, P., A. Catapano, S. M. Bertulli, L. Varesi, R. Fumagalli, and F. Bernini. 1990. Oxidized LDL increase free cholesterol and fail to stimulate cholesterol esterification in murine macrophages. *Biochem. Biophys. Res. Commun.* **171:** 123–131.
57. Gleason, M., M. Meadow, and T. Tulenko. 1991. Excess membrane cholesterol alters calcium movements, cytosolic calcium levels, and membrane fluidity in smooth muscle cells. *Circ. Res.* **69:** 216–217.
58. Feng, B., P. Yao, Y. Li, C. Devlin, D. Zhang, H. Harding, M. Sweeney, J. Rong, G. Kuriakose, E. Fisher, et al. 2003. The endoplasmic reticulum is the site of cholesterol-induced cytotoxicity in macrophages. *Nat. Cell Biol.* **5:** 781–792.
59. Li, Y., M. Ge, L. Ciani, G. Kuriakose, E. Westover, M. Dura, D. Covey, J. Freed, F. Maxfield, J. Lytton, et al. 2004. Enrichment of endoplasmic reticulum with cholesterol inhibits sarcoplasmic-endoplasmic reticulum calcium ATPase-2b activity in parallel with increased order of membrane lipids. *J. Biol. Chem.* **279:** 37030–37039.